Gradient-based controllers for continuous Petri nets

Dimitri Lefebvre, Edouard Leclercq, Fabrice Druaux, Philippe Thomas

Gradient-based controllers for continuous Petri nets

Dimitri Lefebvre, Edouard Leclercq, Fabrice Druaux
Université Le Havre – GREAH, 25 rue P. Lebon, 76063 Le Havre, France
IUT Le Havre – GMP, Place R. Schuman, 76600 Le Havre, France

Philippe Thomas
Centre de Recherche en Automatique de Nancy (CRAN-UMR 7039), Nancy-University, CNRS
ENSTIB 27 rue du Merle Blanc, B.P. 1041, 88051 Epinal cedex 9 France, France

Corresponding author: Pr. Dimitri Lefebvre
Université Le Havre – GREAH, 25 rue P. Lebon, 76063 Le Havre, France
dimitri.lefebvre@univ-lehavre.fr

Abstract*: This paper is about the control design of hybrid dynamical systems modelled with Petri nets. For this purpose, continuous Petri nets with variable speeds are investigated and described as piecewise bilinear state space representations. In this context, the marking vector is considered as a state space vector, subsets of places are defined as the model outputs, and the transitions are divided into non controllable ones and controllable ones that correspond to the model inputs. Gradient-based controllers are proposed and discussed in order to adapt the maximal firing frequencies of the controllable transitions according to desired trajectories of the output markings.*

1. Introduction

Petri nets (PN) are useful for the study of discrete event systems (DES) and hybrid dynamical systems (HDS) (Cassandras 1993, Zaytoon *et al.* 1998) because they combine, in a comprehensive way, intuitive graphical representations and powerful analytic expressions (Brams 1983, Brauer *et al.* 1986, Murata 1989). As a consequence, a lot of results based on PN theory have been established for the control design of DES and HDS. One of the most famous approach concern the supervisory control where the system and the controller are considered as DES (Ramadge *et al.* 1987, Giua *et al.* 1994, Uzam *et al.* 1999). Hybrid approaches were also developed in order to combine discrete and continuous signals (Krogh

et al. 1996, Bemporad *et al.* 1999). At last, continuous approaches were inspired from continuous flow models and continuous Petri nets.

The motivation to use continuous Petri nets is either to model the continuous part of HDS, or to work out a continuous approximation of DES in order to avoid the complexity associated to the exponential growth of states. Flow control design has been developed with different classes of controllers (Silva *et al*. 2003): constrained state feedback (Amrah *et al.* 1996, Lefebvre 1999), fuzzy control (Ghabri 1995), linear programming (Hanzalek 2003), and optimal control (Egilmez *et al.* 1994, Sharifnia A. 1988, 1994). This paper concerns another continuous Petri net approach where the proposed controllers are inspired from the neural network adaptation algorithms (Widrow *et al.* 1990, Thomas 1997) and based on input-output sensitivity functions. For this purpose, continuous Petri nets with variable speeds (VCPN) are investigated and described as piecewise bilinear state space representations where the places marking stands for the state space vector. The system outputs are defined as the marking of subsets of places, and the system inputs correspond to the maximal firing frequencies of a selection of controllable transitions. The main contributions are to investigate the input-output sensitivity of the PN model from structural and also functional points of view. On the one hand, a characterization of input – output structural sensitivity is defined and worked out in a systematic way. On the other hand, sensitivity functions are defined and processed thanks to numerical algorithms that are detailed. As a consequence, gradient-based controllers are proposed in order to adapt the controllable maximal firing frequencies according to desired trajectories of the output markings. The advantages of the gradient-based controllers are pointed out in case of multi-inputs and multi-outputs (MIMO) models for discrete and hybrid systems.

The paper is divided into 5 sections. The section 2 is about PN and VCPN. The section 3 concerns the structural analysis that provides useful results concerning the input-output structural sensitivity. The section 4 is about the design of gradient-based controllers. Various examples of VCPN are proposed in section 5 in order to discuss the proposed results and to compare the gradient-based controllers with proportional and bang-bang ones.

2. Petri nets

A Petri net (PN) with n places and p transitions is defined as $< P, T,$ Pre, Post, $M_0 >$ where $P=\{P_i\}_{i=1,..,n}$ is a not empty finite set of places, $T=\{T_j\}_{j=1,..,p}$ is a not empty finite set of transitions, such that $P \cap T = \varnothing$ (Brams 1983, Murata 1989). IN is defined as the set of integer numbers. Pre: $P \times T \rightarrow IN$ is the pre-incidence application: Pre (P_i, T_j) is the weight of

the arc from place P_i to transition T_j and $W_{PR} = (w^{PR}_{ij})_{i=1,\ldots,n,\ j=1,\ldots,p} \in IN^{n \times p}$ with w^{PR}_{ij} = Pre (P_i, T_j) is the pre-incidence matrix. Post: $P \times T \rightarrow IN$ is the post-incidence application: Post (P_i, T_j) is the weight of the arc from transition T_j to place P_i and $W_{PO} = (w^{PO}_{ij})_{i=1,\ldots,n,\ j=1,\ldots,p} \in IN^{n \times p}$ with w^{PO}_{ij} = Post (P_i, T_j) is the post-incidence matrix. The PN incidence matrix W is defined as $W = W_{PO} - W_{PR} \in IN^{n \times p}$. Let us also define $M = (m_i)_{i=1,\ldots,n} \in IN^n$ as the marking vector and $M_0 \in IN^n$ as the initial marking vector. ${}^{\circ}T_j$ (resp $T_j{}^{\circ}$) stands for the pre-set (resp. post-set) places of T_j. Firing sequences are defined as an ordered series of transitions that are successively fired from marking M to marking M'. Such a sequence is represented by its characteristic vector $X = (x_j)_{j=1,\ldots,p} \in IN^p$ where x_j stands for the number of T_j firings. The marking M' is related to the marking M and to the firing sequence X according to the relation (1):

$$M' = M + W.X. \tag{1}$$

When two transitions T_j and $T_{j'}$ have a common place in the pre-set, the PN presents a structural conflict. The conflict becomes an effective one if there are not enough tokens in the common place to fire both transitions. PN theory does not solve the conflicts. Conflicts are solved according to a decision maker that completes the PN models and that is not considered in this study. In autonomous PN without conflict, the enabling degree of each transition T_j, related to the marking M, is given by equation (2):

$$x_j = \min_{P_i \in {}^{\circ}T_j} \left(fix\left(\frac{m_i}{w^{PR}_{ij}} \right) \right), \tag{2}$$

where fix(.) stands for the integer part of (.).

2.1. Continuous Petri nets

Continuous PN are a particular class of timed PN, deduced from T - timed Petri nets (TPN) (Ramchandani 1973) to provide a continuous approximation of DES behaviour (Alla *et al.* 1999, David *et al.* 1992). A continuous PN with n places and p transitions is defined as < PN, X_{max} > where PN is a Petri net and $X_{max} = (x_{max\ j})_{j=1,\ldots,p} \in IR^{+\,p}$ is the vector of maximal firing frequencies with IR^+ the set of non-negative real numbers The marking $m_i(t)$ of each place P_i, $i = 1,\ldots,n$, at time t has a non-negative real value and each transition firing is a continuous flow in continuous PN. In fact, the transition T_j is fired with a frequency $x_j(t)$ less

than the maximal frequency $x_{max\ j}$. Let us define $X(t) = (x_j(t))_{j=1,\ldots,p} \in IR^{+\ p}$ as the firing frequencies vector at time *t*. The marking evolution is given by the differential system (3):

$$\frac{dM(t)}{dt} = W.X(t). \tag{3}$$

Among the existing models of continuous PN, continuous PN with variable speeds (VCPN), and continuous PN with constant speeds (CCPN) were proved to give good approximations of TPN. In the next sections of this paper, VCPN are preferred because of their interesting properties (David *et al.* 1992): no effective conflict occurs with VCPN; components of the marking vector are continuous functions of the time; components of the firing frequencies vector *X(t)* depend continuously on the marking of the places according to equations (4) and (5):

$$x_j(t) = x_{max\ j}.\mu_j(t), \tag{4}$$

with:

$$\mu_j(t) = \min_{P_i \in {}^{\circ}T_j} \left(\frac{m_i(t)}{w_{ij}^{PR}}\right). \tag{5}$$

Let us also notice that other models of continuous PN were investigated as differential Petri nets (Demongodin *et al.* 1998) or hybrid PN (Zaytoon *et al.* 1998) as illustrated by the example in the next section.

2.2. Continuous PN models of hybrid systems

Continuous PN are suitable to approximate DES or to model the continuous part of HDS (Balduzzi *et al.* 2000, Zaytoon *et al.* 1998) as illustrated with the example in figure 1, modelled with the hybrid PN in figure 2.

[Insert figure 1 about here]

The places P_1 and P_2 are continuous and the markings m_1 and m_2 stand respectively for the height of liquid in tank 1 and tank 2 according to (6):

$$\begin{aligned} S_1.\dot{m}_1 &= x_1 - x_2 - x_3 \\ S_2.\dot{m}_2 &= x_2 + x_3 - x_4 \end{aligned} \tag{6}$$

where S_1 and S_2 stand for the sections of tank 1 and tank 2. The transitions T_1 to T_4 are continuous which firing represents respectively the input flow (T_1), the output flow (T_4) and the flows through the pipes A (T_2) and B (T_3) according to (7):

$$\begin{aligned} x_1 &= D \\ x_2 &= \alpha_2 . \sqrt{m_1 - m_2} \\ x_3 &= \alpha_3 . \sqrt{\sup(m_1, h) - \sup(m_2, h)} \\ x_4 &= \alpha_4 . \sqrt{m_2} \end{aligned} \tag{7}$$

where D, α_2, α_3 and α_4 are related to the system specifications and it is assumed that $m_1 \geq m_2$. The discrete part of the PN (places P_3 and P_4 and transitions T_5 and T_6) stands for the controller. A token in P_3 means that valve V_1 is open and V_2 is closed. On the contrary, a token in P_4 means that valve V_2 is open and V_1 is closed. The arcs from P_1 to T_5 and from P_2 to T_6 are test arcs (the value of the places P_1 and P_2 is not changed by firing the transitions T_5 and T_6). The goal of the controller is to open V_1 and close V_2 when $m_2 < N_2$ and to open V_2 and close V_1 when $m_1 > N_1$. Such a discrete control design results in a cyclic steady state for the continuous variables m_1 and m_2 (figure 17). On the contrary, our approach described in sections 3 and 4 results in continuous control design useful to reach desired levels or to track reference trajectories (figure 18).

[Insert figure 2 about here]

Another example (figure 5) to motivate the use of continuous PN for the modelling and control of HDS will also be considered in the next sections.

2.3. Piecewise bilinear state space representation for VCPN

Due to the commutation function « min » and to the products between marking vector and maximal firing frequencies vector, VCPN models are not linear but piecewise bilinear systems (Amrah *et al.* 1996, Lefebvre 1998, Lefebvre *et al.* 2003a, Lefebvre *et al.* 2004). In order to bring VCPN models in the usual state space representation, let us introduce $U(t) \in IR^{+\,d}$ as the VCPN input vector at time t and $Y(t) \in IR^{+\,q}$ as the VCPN output vector at same instant.

The input vector $U(t)$ is defined as the maximal firing frequencies of the controllable transitions. For this purpose, the set of transitions T is divided into 2 disjoint subsets T_C, and

T_{NC} such that $T = T_C \cup T_{NC}$. T_C is the subset of the controllable transitions, and T_{NC} is the uncontrollable transitions subset. An obvious case is given by $T_C = T$ and $T_{NC} = \varnothing$, but in many cases, not all transitions are controllable. For instance, the transitions T_2 and T_3 in the figure 2, correspond to the flows through the pipes A and B that are not controllable in the sense that these pipes have no valve. As a consequence, let us define $X_C(t) = (x_j(t))_{Tj \in TC} \in IR^{+d}$ and $X_{NC}(t) = (x_j(t))_{Tj \in TNC} \in IR^{+p-d}$ according to (8):

$$D^{-1}.X(t) = \begin{pmatrix} X_C(t) \\ X_{NC}(t) \end{pmatrix}, \tag{8}$$

with $D \in IR^{p \times p}$ a suitable permutation matrix (i.e. D is the matrix of a bijective mapping from T to T that clusters the set of transitions into controllable and uncontrollable ones). The controllable inputs vector $U(t) = X_{max\ C}(t) \in IR^{+d}$ corresponds to the maximal firing frequencies of the transitions to be controlled. The input vector is constrained $0 \le U(t) \le U_{max}$ in order to limit the firing frequencies in a non negative bounded interval. The uncontrollable maximal firing frequencies $X_{max\ NC}$ are supposed to be constant according to the VCPN models.

The output vector $Y(t) = Q.M(t) \in IR^{+e}$ is composed of a selection of subnets markings that are observable. For this purpose, let us define $Q = (q_{ki})_{k=1,\ldots,e\ ,i=1,\ldots,n} \in IR^{e \times n}$ as a positive observation matrix (i.e. Q is the matrix of a constant projector, each row corresponds to a positive weighted sum of the PN places marking). As a consequence, observation may concern not only the marking of some individual places but also the global marking of subsets with several places. The goal of the controller is to drive $Y(t)$ according to some reference trajectories in the output space. Equation (3) can be rewritten as:

$$\begin{aligned} \frac{dM(t)}{dt} &= W_C.X_C(t) + W_{NC}.X_{NC}(t) \\ Y(t) &= Q.M(t) \end{aligned} \tag{9}$$

with $W_C = (w_{C\,ij})_{i=1,\ldots,n,\ j=1,\ldots,d} \in IR^{n \times d}$ and $W_{NC} = (w_{NC\,ij})_{i=1,\ldots,n,\ j=1,\ldots,p-d} \in IR^{n \times (p-d)}$ such that $(W_C \mid W_{NC}) = W.D$.

Several phases occur in the VCPN behaviour (Zehrouni *et al.* 1995). Each phase φ is active between two successive commutations of the “min” operators in (5) and corresponds to a particular configuration of these operators characterised by the p clustering functions f_j:

$$\forall T_j \in T, \quad f_j : IR^{+n} \rightarrow \{1,\ldots,n\}$$

$$M(t) \rightarrow f_j(M(t)) = k \text{ such that } m_k(t) = \mu_j(t). \tag{10}$$

Each function f_j specifies the place in the preset of T_j which has the minimal marking. During each phase φ, a constant relationship between the components of vectors $X_C(t)$ and $M(t)$ and also between $X_{NC}(t)$ and $M(t)$ occurs. This relation can be expressed under scalar form by using the functions f_j or under vectorial form by using the set of vectors $A_j(\varphi) \in \{0,1\}^{1 \times n}$ and $B_j(\varphi) \in \{0,1\}^{1 \times n}$ which are constant during each phase but which may varied from one phase to another:

$$\begin{aligned} x_{C\,j}(t) &= u_j(t).m_{f_j}(t) \\ &= u_j(t).A_j(\varphi).M(t), \qquad j = 1,\ldots d \\ x_{NC\,j}(t) &= x_{\max NCj}.m_{f_j}(t) \\ &= x_{\max NCj}.B_j(\varphi).M(t) \qquad j = 1,\ldots p-d \end{aligned} \tag{11}$$

Equation (8) can be rewritten under scalar form:

$$\begin{aligned} \frac{m_i(t)}{dt} &= \sum_{j=1}^{d} w_{C\,ij}.u_j(t).m_{f_j}(t) + \sum_{j=1}^{p-d} w_{NC\,ij}.x_{\max NC\,j}.m_{f_j}(t) \\ y_k(t) &= \sum_{i=1}^{n} q_{ki}.m_i(t) \end{aligned} \tag{12}$$

or under vectorial form:

$$\begin{aligned} \frac{dM(t)}{dt} &= \left(\sum_{j=1}^{d} u_j(t).W_{Cj}.A_j(\varphi) + \sum_{j=1}^{p-d} x_{\max NC\,j}.W_{NCj}.B_j(\varphi) \right).M(t) \\ Y(t) &= Q.M(t), \end{aligned} \tag{13}$$

where W_{Cj} denotes the j^{th} column of matrix W_C and W_{NCj} denotes the j^{th} column of matrix W_{NC}. Equations (12) and (13) are piecewise bilinear representations of the VCPN (3) (Mohler 1973). Each phase is characterised by a set of matrices $W_{Cj}.A_j(\varphi) \in IN^{n \times n}$ associated to the controllable transitions and $W_{NCj}.B_j(\varphi) \in IN^{n \times n}$ associated to the uncontrollable ones.

The design of gradient-based controllers for VCPN includes structural and functional aspects:

- The structural analysis is necessary to determine which inputs act on a given output. It is also useful to know which outputs are sensitive with respect to the variations of a given input. In section 3, structural sensitivity is defined and structural analysis is discussed.

- The functional analysis consists to adapt the usual gradient algorithm in order to drive the VCPN outputs near the desired marking. In section 4, sensitivity functions are defined and worked out to design gradient - based controllers.

3. Structural analysis

The structural analysis provides qualitative results useful to study the controllability of PN models (Brams 1983, Brauer *et al.* 1986, David *et al*. 1992, Murata 1989, 1977).

3.1. W-sensitivity

This section concerns the structural sensitivity, referred as *W*-sensitivity in the next sections, of the outputs with respect to the variations of the PN inputs. The *W*-sensitivity depends only on the structure of the PN models. As a consequence, the *W*-sensitivity analysis provides controllability properties that are required for the control design of PN and that will be used in section 4. This study is based on the *W*-sensitivity of the places and transitions with respect to the PN firing conditions (Lefebvre 2002, Lefebvre *et al.* 2003b).

Definition 3.1 : The node N (i.e. transition $T_j \in T$ or place $P_i \in P$) is *W*-sensitive with respect to the transition $T_k \in T$ if the firings of T_k could influence the variable attached to N (i.e. the marking m_i of place P_i or the firing x_j of transition T_j). In this case there exists a causality relationship from transition T_k to node N.

The *W*-sensitivity of the outputs with respect to the variations of the PN inputs is defined as a consequence.

Definition 3.2 : The output y_i is *W*-sensitive with respect to the input u_k if a variation of u_k (i.e. the firings of transition $T_k \in T_C$) could influence y_i. In this case there exists a causality relationship from input u_k to output y_i.

The causality relationships can be worked out with the pre and post incidence matrices, according to the theorem 3.1.

Theorem 3.1 : The output y_i is *W*-sensitive with respect to the input u_k if and only if there exists an integer $r \in [0, \min(n, p)]$ such that equation (14) holds:

$$C_i^T.Q.((W_{PR}+W_{PO}).(W_{PR})^T)^r.(W_{PR}+W_{PO}).D.\begin{pmatrix} I_d \\ 0_{p-d} \end{pmatrix}.B_k \neq 0 \quad (14)$$

with $I_d \in IR^{d\,x\,d}$ the identity matrix, $0_{p\text{-}d} \in IR^{(p\text{-}d)\,x\,d}$ the zeros matrix, $B_k = (b^k_j) \in \{0, 1\}^d$ such that $b^k_j = 0$ if $k \neq j$ and $b^k_k = 1$, and $C_i = (c^i_j) \in \{0, 1\}^q$ such that $c^i_j = 0$ if $i \neq j$ and $c^i_i = 1$.

Proof : A perturbation of the firing conditions of transition T_k yields a deviation of the places marking next to T_k ($^\circ T_k \cup T_k^\circ$) from its true value. This deviation is likely to change the firing of the downstream transitions (($^\circ T_k \cup T_k^\circ$)$^\circ$). In fact, the initial perturbation could propagate in the PN according to the following rules.

1) A perturbation of the firing conditions of transition T_k yields a deviation of the T_k - input and T_k - output places marking ($^\circ T_k \cup T_k^\circ$) from its true value. But the perturbation could influence the firing conditions of T_j only if the T_j - input places ($^\circ T_j$) marking is modified.

[Insert figure 3 about here]

2) A deviation of the marking of the place P_i influences the firing conditions of the P_i – downstream transitions (P_i°). But the marking of the place P_i has a structural sensitivity with respect to the P_i - upstream and P_i - downstream transitions ($^\circ P_i \cup P_i^\circ$).

[Insert figure 4 about here]

The characterisation of the neighbourhood in PN results from the algebraic properties of the post and pre incidence matrices:

- The position of the non-zero entries of the j^{th} column in W_{PR} (resp. in W_{PO}) corresponds to the T_j - input places (resp. T_j - output places).
- The position of the non-zero entries of the i^{th} row in W_{PR} (resp. in W_{PO}) corresponds to the P_i - downstream transitions (resp. P_i - upstream transitions).
- The position of the non-zero entries of the j^{th} column in $W_{PR} + W_{PO}$ (resp. the i^{th} row in $W_{PR} + W_{PO}$) corresponds to the places (resp. transitions) next to T_j (resp. P_i).

The set of places that are structurally sensitive with respect to the firing conditions of $T_k \in T_C$ is worked out with a recursive algorithm. The position of the non-zero entries of the k^{th} column in $W_{PR} + W_{PO}$ corresponds to the places next to T_k. The position of the non-zero entries of the k^{th} column in $(W_{PR})^T.(W_{PR} + W_{PO})$ corresponds to the downstream transitions

next to the places next to T_k. The position of the non-zero entries of the k^{th} column in $(W_{PR} + W_{PO}).(W_{PR})^T.(W_{PR} + W_{PO})$ corresponds to the places next to the downstream transitions next to the places next to T_k, and so on. When the PN has n places and p transitions, the structural sensitivity analysis of the places and transitions is completed in a finite number of steps no larger than min(n, p). The output y_i is W - sensitive with respect to $T_k \in T_C$ if at least one place of the subnet y_i is sensitive with respect to T_k. The permutation matrix D and projector Q are used to limit the neighbourhood characterization to the controllable transitions and output subnets.

Definition 3.3 : The matrix $S_W = (s_W(y_i, u_k))_{i = 1,\ldots,q,\ k = 1,\ldots,d} \in \{[0, min(n,p)] \cup \infty\}^{q \times d}$ is defined as the input-output W-sensitivity matrix where $s_W(y_i, u_k)$ is given by equation (15):

$$sw(y_i, u_k) = \min_{r \in [0,\ \min(n,p)] \cup \infty} \left\{ C_i^T.Q.((W_{PR} + W_{PO}).(W_{PR})^T)^r.(W_{PR} + W_{PO}).D.\begin{pmatrix} I_d \\ 0_{p-d} \end{pmatrix}.B_k \neq 0 \right\} \qquad (15)$$

$s_W(y_i, u_k)$ equals either infinity if y_i is not W-sensitive with respect to the input u_k, and no causality relationship exists from u_k to y_i, or the number of intermediate places in the shortest causality relationship (Lefebvre *et al.* 2003b) from u_k to y_i if y_i is W-sensitive with respect to the input u_k. In this last case, $s_W(y_i, u_k)$ is named the W-sensitivity rank of y_i with respect to u_k. The W-sensitivity matrix provides immediate results about the causality relationships in PN, as explained in theorem 3.2:

Theorem 3.2:

The set of outputs (resp. rank - r outputs) that are W - sensitive with respect to the input u_k is given by the position of the finite entries (resp. entries with value r) of the k^{th} column in matrix S_W .

The set of inputs (resp. rank – r inputs) whose firing conditions are likely to influence the output y_i is given by the position of the finite entries (resp. entries with value r) of the i^{th} row in matrix S_W.

Proof : the proof of theorem 3.2 is obvious and results from definition 3.2 and theorem 3.1.

As a conclusion, let us notice that the causality relationships do not coincide with directed paths (see, for example, system B and equation (19): $s_W(P_1, T_2) = 1$, but the shortest directed

path from T_2 to P_1 is of length 2). Let us also emphasis the fact that the *W*-sensitivity is not restricted to a specific class of PN. In fact the *W*-sensitivity concerns all classes of PN that result from the basic relationship (1).

3.2. Examples

In order to illustrate the *W* – sensitivity analysis, the following examples are proposed.
The VCPN B with the marking vector $M(t) = (m''_0(t), m''_1(t), m''_2(t), m_1(t), m_2(t), m'_1(t), m'_2(t))^T$ shown in figure 5 is the model of a manufacturing process with 2 machines M_1 and M_2 corresponding to the 2 transitions T_1 and T_2. Machines are fed by buffers with limited capacities corresponding to the subsets of places $\{P_1, P'_1\}$ and $\{P_2, P'_2\}$ (Amrah *et al.* 1996).

[Insert figure 5 about here]

The maximal capacities C_1 and C_2 of the buffers correspond to the initial marking $m_1(0) + m'_1(0) = C_1$ and $m_2(0) + m'_2(0) = C_2$. Pieces enter in the system by firing T_0. The number of pieces that are simultaneously processed by each machine is bounded by the marking of the places P''_0, P''_1, and P''_2. (i.e. an initial marking $m''_i(0) = 1$, $i = 1,\ldots,3$ stands for single servers and $m''_i(0) > 1$ stands for multi servers). The continuous behaviour of this system is given by equation (16):

$$\begin{aligned}
\dot{m}_1(t) &= x_{\max 0}.\min(m''_0(t), m'_1(t)) - x_{\max 1}.\min(m''_1(t), m_1(t), m'_2(t)) \\
\dot{m}_2(t) &= x_{\max 1}.\min(m''_1(t), m_1(t), m'_2(t)) - x_{\max 2}.\min(m''_2(t), m_2(t))
\end{aligned}$$

$$\begin{aligned}
m'_i(t) &= C_i - m_i(t) && i = 1,2 \\
m''_j(t) &= m''_j(0) && j = 1,2,3
\end{aligned} \qquad (16)$$

The set of controllable transitions and the set of outputs subnets depend on system specifications. Let us first consider the system (16) as a single input – multi outputs one and assume that $T_C = \{T_0\}$ and $T_{NC} = \{T_1, T_2\}$, then $u(t) = x_{max\ 0}(t)$. Let us also assume that $y_1(t) = m_1(t)$, and $y_2(t) = m_2(t)$. Other specifications are discussed in the following. The VCPN (16) can be written as a scalar form (17) by using the functions f_j defined as in (10):

$$\begin{aligned}
\dot{m}_1(t) &= u(t).m_{f0}(t) - x_{\max 1}.m_{f1}(t) \\
\dot{m}_2(t) &= x_{\max 1}.m_{f1}(t) - x_{\max 2}.m_{f2}(t) \\
y_1(t) &= m_1(t), \qquad y_2(t) = m_2(t)
\end{aligned} \qquad (17)$$

or as a vectorial form (18):

$$\begin{aligned} \dot{M}(t) &= (u(t).W_{C1}.A_1(\varphi) + x_{\max 1}.W_{NC1}.B_1(\varphi) + x_{\max 2}.W_{NC2}.B_2(\varphi)).M(t) \\ Y(t) &= Q.M(t) \end{aligned} \quad (18)$$

with W_{C1} = (0, 0, 0, 1, 0, -1, 0)^T, W_{NC1} = (0, 0, 0, -1, 1, 1, -1)^T, W_{NC2} = (0, 0, 0, 0, -1, 0, 1)^T, Q = ((0 0 0 1 0 0 0)^T; (0 0 0 0 1 0 0)^T)^T. The row vectors $A_1(\varphi)$, $B_1(\varphi)$, and $B_2(\varphi)$ depend of the current phase (table 1). For example, if $M = M_0$, these row vectors are $A_1(\varphi)$ = (1, 0, 0, 0, 0, 0, 0), $B_1(\varphi)$ = (0, 0, 0, 1, 0, 0, 0), and $B_2(\varphi)$ = (0, 0, 0, 0, 1, 0, 0).

[Insert table 1 about here]

The *W*-sensitivity matrix of the PN places with respect to the transitions is given by $S_W(P,T)$ and the *W*-sensitivity matrix of the PN outputs with respect to the single input is given by $S_W(Y,U)$ according to equation (19):

$$S_W(P,T) = \begin{array}{c} \begin{matrix} T_0 & T_1 & T_2 \end{matrix} \\ \begin{pmatrix} 0 & 1 & 2 \\ 1 & 0 & 1 \\ 2 & 1 & 0 \\ 0 & 0 & 1 \\ 1 & 0 & 0 \\ 0 & 0 & 1 \\ 1 & 0 & 0 \end{pmatrix} \end{array} \begin{matrix} P''_0 \\ P''_1 \\ P''_2 \\ P_1 \\ P_2 \\ P'_1 \\ P'_2 \end{matrix} \qquad S_W(Y,U) = \begin{array}{c} u \\ \begin{pmatrix} 0 \\ 1 \end{pmatrix} \end{array} \begin{matrix} y_1 \\ y_2 \end{matrix} \quad (19)$$

The *W*-sensitivity matrix $S_W(P, T)$ shows that the marking of each place depends on the firing of all transitions: the content of each intermediate buffer depends of the production rate of upstream but also downstream machines. These causality relationships concern the immediate neighbourhood when $S_W(P_i,T_j) = 0$ or non immediate neighbourhood when $S_W(P_i,T_j) > 0$. The same conclusions can be driven concerning the input – output *W*-sensitivity matrix $S_W(Y, U)$.
The table 2 provides the W-sensitivity matrices of the output(s) with respect to the input(s) for several set of controllable transitions and several output subnets.

[Insert table 2 about here]

The investigation of the input – output causality relationships is useful in order to design efficient control. For instance, if the controller goal is that the content of the first intermediate buffer reaches a desired level or tracks a desired trajectory, it is more convenient to control the input transition T_0 ($S_W(y = m_1, u = x_{max\ 0}) = 0$), than the transition T_2 ($S_W(y = m_1, u = x_{max\ 2}) = 1$). Such a conclusion will be confirmed in section 4.

The results obtained with the structural analysis can be more definitive as shown with a simple modification of the previous example. The system is changed in the sense that the intermediate buffers have an infinite capacity according to figure 6 and equation (20):

[Insert figure 6 about here]

$$\dot{m}_1(t) = x_{\max 0}.m''_0(t) - x_{\max 1}.\min(m''_1(t), m_1(t))$$
$$\dot{m}_2(t) = x_{\max 1}.\min(m''_1(t), m_1(t)) - x_{\max 2}.\min(m''_2(t), m_2(t))$$

$$m''_j(t) = m''_j(0) \qquad j = 1,2,3 \tag{20}$$

With the same specification as previously, the transitions - places *W*-sensitivity matrix $S'_W(P,T)$ and the input – output *W*-sensitivity matrix $S'_W(Y,U)$ are given by (21):

$$S'_W(P_i,T_j) = \begin{array}{c} \\ P''_0 \\ P''_1 \\ P''_2 \\ P_1 \\ P_2 \end{array} \begin{array}{c} \begin{array}{ccc} T_0 & T_1 & T_2 \end{array} \\ \begin{pmatrix} 0 & \infty & \infty \\ 1 & 0 & \infty \\ 2 & 1 & 0 \\ 0 & 0 & \infty \\ 1 & 0 & 0 \end{pmatrix} \end{array} \neq S_W(P_i,T_j) \qquad S'_W(Y,U) = \begin{array}{c} u \\ \begin{pmatrix} 0 \\ 1 \end{pmatrix} \end{array} \begin{array}{c} y_1 \\ y_2 \end{array} = S_W(Y,U) \tag{21}$$

The table 3 that provides the *W*-sensitivity matrices of the output(s) with respect to the input(s) for several sets of controllable transitions and several output subnets must be compared with table 2.

[Insert table 3 about here]

From table 3, it is obvious that transition T_2 can no more be used to control the output $y(t) = m_1(t)$: there exist no causality relationship from T_2 to P_1 because of the infinite capacity buffer represented by P_2.

Another example of generalised VCPN is given by system C in figure 7 with the marking vector $M(t) = (m'_1(t), m'_2(t), m'_3(t), m'_4(t), m'_5(t), m_1(t), m_2(t), m_3(t), m_4(t))^T$. Weighted arcs T_2 -> P_1 and P_1 -> T_1 means that the flow of tokens that fire T_2 to P_1 is multiplied by 3 and the flow of tokens that fire T_1 from P_1 is divided by 2. As previously, places P'_1 to P'_5 limit the number of simultaneous firings of the transitions T_1 to T_5. The set of controllable transitions is assumed to be given as $T_C = \{T_4, T_5\}$ and the set of non controllable transitions is given by $T_{NC} = \{T_1, T_2, T_3\}$. In this case, the controllable transitions correspond to source transitions that represent the interface between the system and the "outside word" and the set of non controllable transitions corresponds to internal transitions that are assumed to behave according to their own dynamic. The maximal firing frequencies of the internal transitions is given by $X_{max\ NC} = \{2, 1, 3\}$. The output subnets are defined according to $\{P_1, P_3\}$ and $\{P_2, P_4\}$ (i.e. $y_1(t) = m_1(t) + m_3(t)$ and $y_2(t) = m_2(t) + m_4(t)$).

[Insert figure 7 about here]

This VCPN can be written as a scalar form (22) or as a vectorial form (23):

$$\begin{aligned}
\dot{m}_1(t) &= u_1(t).m_{f4}(t) + 3.x_{\max 2}.m_{f2}(t) - 2.x_{\max 1}.m_{f1}(t) \\
\dot{m}_2(t) &= u_2(t).m_{f5}(t) + x_{\max 3}.m_{f3}(t) - x_{\max 1}.m_{f1}(t) \\
\dot{m}_3(t) &= x_{\max 1}.m_{f1}(t) - x_{\max 2}.m_{f2}(t) \\
\dot{m}_4(t) &= x_{\max 1}.m_{f1}(t) - x_{\max 3}.m_{f3}(t)
\end{aligned} \qquad (22)$$

$$\begin{aligned}
y_1(t) &= m_1(t) + m_3(t) \\
y_2(t) &= m_2(t) + m_4(t)
\end{aligned}$$

Let us mention that the functions f_4 and f_5 are constant and $m_{f4}(t) = m_{f5}(t) = 1$, because the controllable transitions are source transitions.

$$\begin{aligned}
\dot{M}(t) = (&u_1(t).W_{C1}.A_1(\varphi) + u_2(t).W_{C2}.A_2(\varphi) \\
&+ x_{\max 1}.W_{NC1}.B_1(\varphi) + x_{\max 2}.W_{NC2}.B_2(\varphi) + x_{\max 3}.W_{NC3}.B_3(\varphi)).M(t) \\
Y(t) &= Q.M(t)
\end{aligned} \qquad (23)$$

with $W_{C1} = (0, 0, 0, 0, 0, 1, 0, 0, 0)^T$, $W_{C2} = (0, 0, 0, 0, 0, 0, 1, 0, 0)^T$, $W_{NC1} = (0, 0, 0, 0, 0, -1, -1, 1, 1)^T$, $W_{NC2} = (0, 0, 0, 0, 0, 1, 0, -1, 0)^T$, $W_{NC3} = (0, 0, 0, 0, 0, 0, 1, 0, -1)^T$, $A_1(\varphi)$, $A_2(\varphi)$, $B_1(\varphi)$, $B_2(\varphi)$, and $B_3(\varphi)$ that depend of the current phase, and $Q = ((0\ 0\ 0\ 0\ 0\ 1\ 0\ 1\ 0)^T; (0\ 0\ 0$

$0\ 0\ 0\ 1\ 0\ 1)^T)^T$. The input-output *W*-sensitivity matrix (24) shows that both outputs are correlated according to the transition T_1.

$$S_W(Y,U) = \begin{array}{c} \begin{matrix} u_1 & u_2 \end{matrix} \\ \begin{pmatrix} 0 & 1 \\ 1 & 0 \end{pmatrix} \end{array} \begin{array}{l} y_1 \\ y_2 \end{array} \tag{24}$$

4. Control design for VCPN

Flow control for VCPN was investigated by several authors (Amrah *et al.* 1996, Egilmez *et al.* 1994, Ghabri 1995, Hanzalek 2003, Lefebvre 1999, Silva *et al*. 2003). Such methods have provided interesting results but require strong conditions concerning the transitions to control and the places to observe. Moreover, the proposed results are often local ones, and are attached to a specific phase in the VCPN behaviour. This paper focus on another approach based on gradient method and inspired from neural networks. Gradient-based methods have been intensively investigated for the learning of neural networks (Widrow *et al.* 1990) and the identification of continuous systems (Ljung 1987, Thomas 1997) but only a few studies have concerned the hybrid and discrete event systems (Balduzzi *et al.* 2000). This approach takes advantages on the propagation of the gradient through the PN nodes in order to minimise the square of instantaneous error between desired and measured outputs by modifying the maximal firing frequencies of controllable transitions. Gradient algorithms perform the minimisation of a scalar cost function that evaluates the distance between the desired output $Y_d(t)$ and the system output $Y(t)$. Let us assume that measurements of the desired output are obtained with a sampling period Δt during the time horizon H. As a consequence, the proposed controllers will be worked out in discrete time.

4.1 Sensitivity functions

Gradient algorithms are based on the evaluation of sensitivity functions. Such functions are defined in continuous time for VCPN (definition 4.1) and will be worked out in discrete time (theorem 4.1) according to the sampling period Δt in order to be implemented in numerical controllers.

Definition 4.1: The scalar sensitivity function $s_{\alpha\gamma}(t)$ for the output y_α with respect to the input u_γ and the sensitivity function vector $S_\alpha(t)$ for the output y_α with respect to the input vector U are defined as:

$$s_{\alpha\gamma}(t) = \frac{\partial y_\alpha}{\partial u_\gamma} \in IR\,, \qquad S_\alpha(t) = (s_{\alpha\gamma}(t))_{\gamma=1,..,d} = \left(\frac{\partial y_\alpha}{\partial u_\gamma}\right)_{\gamma=1,..,d} \in IR^d \tag{25}$$

Theorem 4.1: The numerical process given by equation (26) tends to the value of the scalar sensitivity function $s_{\alpha\gamma}(t)$ worked out at time $t = k.\Delta t$:

$$\delta s_{\alpha\gamma}(k) = \sum_{i=1}^{n} q_{\alpha i} . \left(w_{i\gamma} . \mu_\gamma(k) + \sum_{\substack{j=1 \\ j\neq\gamma}}^{p} w_{ij} . x_{\max j} . s_{fj\,\gamma}(k) \right) . \Delta t \tag{26}$$

with $\delta s_{\alpha\gamma}(k) = s_{\alpha\gamma}(k) - s_{\alpha\gamma}(k\text{-}1)$ and $s_{\alpha\gamma}(0) = 0$.

Proof : Let us first notice that the sensitivity functions can be formulated in terms of the VCPN marking and of the transitions maximal firing frequency at time $t = k.\Delta t$:

$$s_{\alpha\gamma}(k) = \left(\frac{\partial y_\alpha}{\partial u_\gamma}\right)_{\substack{y_\alpha = y_\alpha(k.\Delta t) \\ u_\gamma = u_\gamma(k.\Delta t)}} = \sum_{i=1}^{n} q_{\alpha i} . \left(\frac{\partial m_i}{\partial x_{\max\gamma}}\right)_{t=k.\Delta t} \tag{27}$$

According to the equations (3), (4) and (5):

$$\frac{\partial}{\partial x_{\max\gamma}} \left(\frac{dm_i(t)}{dt}\right) = \sum_{j=1}^{p} w_{ij} . \frac{\partial x_j(t)}{\partial x_{\max\gamma}} = w_{i\gamma} . \mu_\gamma(t) + \sum_{\substack{j=1 \\ j\neq\gamma}}^{p} w_{ij} . x_{\max j} . \frac{\partial \mu_j(t)}{\partial x_{\max\gamma}} \tag{28}$$

Using the clustering functions defined as in (10), equation (28) results in (29):

$$\frac{\partial}{\partial x_{\max\gamma}} \left(\frac{dm_i(t)}{dt}\right) = w_{i\gamma} . \mu_\gamma(t) + \sum_{\substack{j=1 \\ j\neq\gamma}}^{p} w_{ij} . x_{\max j} . s_{fj\gamma}(t) \tag{29}$$

The derivation with respect to time of the sensitivity functions (25) and the use of a first order numerical method leads to equation (26).

4.2 Gradient-based controllers

For the seek of simplicity, let us first consider the single output case. The instantaneous error is defined as $\varepsilon(k,i) = y_d(k) - y(k,i)$, where $y_d(k)$ stands for the desired output at time $t = k.\Delta t$, and $y(k,i)$ stands for the marking of the VCPN output y at time $t = k.\Delta t$ obtained from the marking $M(k-1)$ and the input vector $U(k-1,i)$ according to a first order numerical method:

$$y(k,i) = y(k-1) + \Delta t.(\sum_{j=1}^{d} u_j(k-1,i).Q.W_{Cj}.A_j(\varphi) + \sum_{j=1}^{p-d} x_{\max NC\ j}.Q.W_{NCj}.B_j(\varphi)).M(k-1) \tag{30}$$

$U(k,i)$ is the updating of the input vector obtained after the i^{th} iteration of the gradient algorithm at time $t = k.\Delta t$. A maximal number of N iterations is considered, for each instant $t = k.\Delta t$, in order to work out the input $U(k)$ in finite time. According to this truncation, we have $U(k) = U(k, N)$, and $y(k) = y(k, N)$. Let us consider the scalar cost function $v(k, i)$:

$$v(k,i) = \frac{1}{2}\varepsilon^2(k,i) \in IR. \tag{31}$$

Gradient-based methods result from the Taylor series expansion of the cost function $v(k, i)$ in order to work out the optimal value of the input vector $U(k, i)$:

$$\begin{aligned} v(k,i+1) &= v(k,i) + \left(\frac{\partial v}{\partial U}\right)^T_{U=U(k,i)} \delta U(k,i) \\ &+ \frac{1}{2}.(\delta U(k,i))^T \left(\frac{\partial^2 v}{\partial U.\partial U^T}\right)_{U=U(k,i)} \delta U(k,i) + o(\left|\delta U(k,i)^T.\delta U(k,i)\right|) \end{aligned} \tag{32}$$

with $\delta U(k,i) = U(k,i+1) - U(k,i)$. The stationary condition results in:

$$\delta U(k,i) = -\left(\frac{\partial^2 v}{\partial U.\partial U^T}\right)^{-1}_{U=U(k,i)}.\left(\frac{\partial v}{\partial U}\right)_{U=U(k,i)} \tag{33}$$

with:

$$\left(\frac{\partial v}{\partial U}\right)_{U=U(k,i)} = -S(k).\varepsilon(k,i)$$

$$\left(\frac{\partial^2 v}{\partial U.\partial U^T}\right)_{U=U(k,i)} \approx \left(\frac{\partial^2 v}{\partial U.\partial U^T}\right)_{U=U(k-1)} \approx S(k).S(k)^T + \alpha I \tag{34}$$

S(k) is the output sensitivity function vector of output *y* with respect to the input vector *U* defined as in (25) and worked out at time $t = k.\Delta t$ according to equation (26). Let us notice that the sensitivity functions do not depend on the iteration *i*. *S(k)* is computed a single time for each new measurement. Moreover, second order terms are usually neglected in equation (33), but an adaptive term $\alpha.I$ is added in order to approximate the inverse of the Hessien matrix when it is not regular or badly conditioned (Hagan *et al.* 1995). Thus, equation (33) results in the updating rule of the controller (35):

$$\begin{aligned} &\delta U(k,i) = (S(k).S(k)^T + \alpha.I)^{-1}.S(k).\varepsilon(k,i),\ i = 0,...,N-1 \\ &U(k,0) = U(k-1) \end{aligned} \tag{35}$$

Let us point out two limit cases. When $\alpha >> 1$, equation (35) corresponds to the gradient method (Van der Smagt *et al.* 1994):

$$\delta U(k,i) = \frac{1}{\alpha}.S(k).\varepsilon(k,i)\,. \tag{36}$$

When $\alpha << 1$, equation (35) corresponds to the Gauss-Newton method (Thomas 1997):

$$\delta U(k,i) = (S(k).S(k)^T)^{-1}.S(k).\varepsilon(k,i)\,. \tag{37}$$

The previous controller can be generalised in the multi-outputs case, by considering the scalar cost function (38):

$$v(k,i) = \frac{1}{2}.\sum_{j=1}^{q} \varepsilon_j{}^2(k,i) \in IR \tag{38}$$

that results in the following updating rule for the controller:

$$\begin{aligned} &\delta U(k,i) = (\sum_{j=1}^{q}(S_j(k).S_j(k)^T + \alpha.I))^{-1}.(\sum_{j=1}^{q} S_j(k).\varepsilon_j(k,i)) \\ &U(k,0) = U(k-1) \end{aligned} \tag{39}$$

where $S_j\ (k)$ stands for sensitivity function vector of the output y_j with respect to the input vector U at time $t = k.\Delta t$.

5. Examples

In order to illustrate the proposed controllers, let us first consider the system B modelled as a VCPN where the incidence matrices and parameters are defined as in section 3. The piecewise bilinear state space representation of system B is given by equation (18) with constrained input limited to 5 tokens /UT. The initial marking vector is M_0 = (1 1 1 0 0 3 3) and the parameter α equals 0,1 in order to avoid the singularities in the Hessien approximation (34).
The figure 8 illustrates the equilibriums for system B in the plan (m_1, m_2) obtained for the same sets of controllable transitions : $T_C = \{T_0\}$, $T_C = \{T_2\}$, or $T_C = \{T_0, T_2\}$ that were investigated in section 3 (in black: without control, in light grey: with constant control, in dark grey: reachable equilibriums from the origin with constant control). Let us mention that the region of reachable equilibriums from the origin with constant control is always strictly included in the region of the system equilibriums obtained for all admissible initial markings $0 \leq m_1(0) \leq 3$ and $0 \leq m_2(0) \leq 3$.

[Insert figure 8 about here]

Let us first consider the case $T_C = \{T_0\}$. The figure 9 points out the influence of the output matrix on the controller response: 3 scalar outputs are investigated $y = m_1$, $y = m_2$ and $y = m_1 + m_2$ that correspond respectively to Q_1 = (0 0 0 1 0 0 0), Q_2 = (0 0 0 0 1 0 0), Q_3 = (0 0 0 1 1 0 0). In all cases, the objective of the controller is to drive the output of the system to the desired value y_d = 2 tokens. The maximal number of iterations is N = 100. Concerning the output matrices Q_2 and Q_3 the desired value is rapidly reached with a good accuracy, but in case of output matrix Q_1 some oscillations are observed. Such an input – output specification is not suitable with our approach because the marking of the unobservable place P_1 is not considered in the calculation of the input firing frequency. As a consequence, the desired level is exceeded and oscillations arise due to the delay between the firing of T_0 and the observation of P_2 marking. In order to avoid the undesirable cumulative effects of the marking, the inputs and outputs of the systems must be preferred such that the sensitivity rank equals 0 (immediate neighbourhood) as shown in table 2.

[Insert figure 9 about here]

The speed of the algorithm increases as the maximal number of iterations in the gradient – based algorithm. The figure 10 illustrates the influence of the number of iterations N when the output matrix is given by Q = (0 0 0 1 0 0 0). A small number (N = 2 or N = 10) results in a poor controller, that is not quick enough to correct the input when the desired level is reached. In this case the level is exceeded and there is nothing to do. A large number (N = 100) compensates the slowness of the gradient algorithm.

[Insert figure 10 about here]

In figures 11 and 12, gradient-based controllers (full line) with $T_C = \{T_0\}$, N = 100 and Q = (0 0 0 1 1 0 0) are compared with usual proportional (dashed line) and bang-bang controllers (dotted line) when the desired output is the piecewise linear function of time given by equation (31) (figure 11):

$$\begin{cases} y_d = \frac{t}{3}, \ 0 \le t < 6 \\ y_d = \frac{1}{9}.t + \frac{4}{3}, \ t \ge 6 \end{cases} \tag{31}$$

or a C^0 non linear function of time given by equation (32) (figure 12):

$$y_d = \left|\sin(t)\right| + \frac{t}{6} \tag{32}$$

All proposed controllers track the desired trajectories with an instantaneous error that does not exceed 0.5 token ($\varepsilon < 0.2$ tokens for the proportional controller, $\varepsilon < 0.4$ tokens for the bang-bang controller, $\varepsilon < 0.05$ tokens for the gradient-based controller). Let us notice that the error of the gradient-based controller is smaller than the one of the proportional or the bang-bang controller. Furthermore, the input signal is very different according to the controller choice. The proportional controller uses the error signal as the input frequency (gain = 1). As a consequence, this controller is not suitable when the error signal presents a lot of variations. The bang-bang controller is defined as a series of commutations. The input flow of tokens is tuned according to the commutations frequency. For this reason, the interest of this controller depends strongly of the field of application. The most outstanding difference between the different classes of controllers is that only the gradient-based controller is able to learn the

growing rate of the output in the case of a linear trajectory and the cyclic behaviour of the output in the case of a non linear sinusoidal trajectory.

[Insert figures 11 and 12 about here]

Let us now consider the VCPN model of system C (figure 7) given as a MIMO piecewise bilinear state space representation (23) with inputs that correspond to T_C = {T_4, T_5} and outputs that correspond to the subsets {P_1, P_3} and {P_2, P_4}. The firing of controllable transitions is limited to 5 tokens /UT, the initial marking vector is $M_0 = (1\ 1\ 1\ 1\ 1\ 0\ 0\ 0\ 0)^T$, the parameter α equals 0.1, and the number of iterations is limited to N = 100. The desired trajectories correspond to 2 piecewise linear trajectories given by equation (33):

$$\begin{cases} y_{d1} = \frac{5}{3}.t, & 0 \le t < \frac{12}{5} \\ y_{d1} = \frac{5}{24}.t + \frac{7}{2}, & t \ge \frac{12}{5} \end{cases} \qquad \begin{cases} y_{d2} = t, & 0 \le t < 6 \\ y_{d2} = \frac{1}{3}.t + 4, & t \ge 6 \end{cases} \tag{33}$$

Only the outputs of the gradient-based controller are presented in figure 13. In fact the proportional and bang-bang controllers provide only poor results because the inputs and outputs of the system C are coupled thanks to the transition T_1. These controllers focus on one desired trajectory but cannot track simultaneously both ones. On the contrary, the gradient-based controller tracks simultaneously both trajectories with an instantaneous error that does not exceed 0,2 tokens. The input-output decomposition is obtained thanks to the sensitivity functions that evaluate for each output the relative influence of both inputs.

[Insert figure 13 about here]

The figure 15 illustrates the case of a non admissible output trajectory. The desired output signals are defined as previously but the incidence relationships of the VCPN have been modified according to figure 14 (system C'):

[Insert figure 14 about here]

System C is tokens consumer but system C' is tokens producer: the free response ($U(t)$ = 0) of system C' corresponds to increasing marking functions whereas the free

response of system C corresponds to a decreasing marking functions. After t = 4 TU, we have $u_1(t)$ = 0, but the number of tokens in subnet y_2 increases more quickly than the desired output y_{d2} and the controller fails.

[Insert figure 15 about here]

At last, let us consider the hybrid PN model of the two tanks system A (figure 1) given as a MIMO non linear state space representation which inputs correspond to the maximal firing frequencies of the controllable transitions $T_C = \{T_1, T_4\}$ and outputs correspond to the marking m_1 and m_2. The controller is obtained according to an adaptation of the gradient based algorithm to non linear behaviours. As a consequence, the discrete part of the hybrid model become useless (figure 2). The firing of controllable transitions is limited according to the system specifications : $0 \leq u_1 \leq D$, and $0 \leq u_2 \leq \alpha_4$, with $\alpha_2 = \alpha_3 = \alpha_4 = 1.6.10^{-4}$ $m^{3/2}.s^{-1}$, $D = 1.10^{-4}$ $m^3.s^{-1}$, h = 0.5 m, $S_1 = S_2 = 0.0154$ m^2. The initial marking vector of the continuous part of the model is M_0 = (0, 0); the coefficient α equals 0,1; the number of iterations is limited to N = 1 (single step controller). The desired trajectories correspond to a periodical level for tank 1 and a constant level for tank 2. Simulation results for the gradient based controller are given in figure 16 (system outputs are in full line, and desired trajectories are in dotted line) and can be compared with the results obtained with the discrete control design (figure 17).

[Insert figures 16 and 17 about here]

Both controllers are different in terms of objective. Nevertheless, one can notice that the discrete controller is not suitable to track some reference trajectories or to reach some desired levels. On the contrary, with gradient – based controller, the desired level in tank 2 is reached and the reference trajectory in tank 1 is almost everywhere tracked after some transitory behaviours. But one can also notice that, due to system specifications, level 0.6 m cannot be reached in tank 1 when level in tank 2 is 0.4 m. In fact, the desired levels m_{1d} = 0.6 m and m_{2d} = 0.4 m do not belong to the set of equilibriums. At last, because of immediate causality relationships from T_1 to P_1 and from T_4 to P_2, the gradient – based algorithm behaves like a proportional controller (i.e. the input – output sensitivity matrix tends to a diagonal one).

6. Conclusions

The continuous Petri net controllers that have been proposed in this paper are based on the evaluation of the input-output sensitivity functions. For this purpose, the structural sensitivity of PN models has been first investigated. Places to be observed and transitions to be controlled are obtained as a consequence. An explicit characterisation of the input-output sensitivity functions has also been proposed for VCPN models. At last, VCPN controllers have been designed that calculate the gradient of the outputs with respect to the input variations in order to adapt the maximal firing frequencies of the controllable transitions according to desired trajectories of the output markings. An adaptation of this algorithm for HDS and continuous non linear PN was also developed.

In our opinion, the method is not only suitable for trajectory tracking but also for complex behaviours learning. We will further investigate the combination of Petri nets and neural networks in order to design learning Petri nets (Hirasawa *et al.* 1998). These perspectives include not only the continuous Petri nets but also the autonomous and timed Petri nets. At last, the sensitivity analysis will also be adapted for the monitoring of hybrid systems modelled with Petri nets.

7. References

Alla A., David R., 1999, Continuous and hybrid Petri nets, *Journal of Circuits, Systems, Computers*, vol. 8, n°. 1, pp 159 – 188.

Amrah A., Zerhouni N., El Moudni A., 1996, Constrained state feedback control of a class of discrete event systems modelled by continuous Petri nets, *ICARCV 96 Proceedings*, pp. 979-984, Singapore.

Balduzzi F., Giua A., Menga G., 2000, First-order hybrid Petri nets: a model for optimization and control, *IEEE Trans. On Robotics and Automation*, vol. 16, no. 4, pp. 382 –399.

Bemporad A., Morari M., 1999, Control of systems integrating logic, dynamics and constraints, *Automatica*, vol. 35, no. 11, pp. 407 – 427.

Brams G.W., 1983, *Réseaux de Petri*, Vol I et II, Masson, Paris.

Brauer W., Reisig W., Rozenberg G., 1986, Petri nets: Central models and their properties, *Lecture Notes in Computer Science*, vol. 254, Springer Verlag.

Cassandras C.G., 1993, *Discrete event systems: modeling and performances analysis*, Aksen Ass. Inc. Pub.

David R., Alla H, 1992, *Petri nets and grafcet – tools for modelling discrete events systems*, Prentice Hall, London.

Demongodin I., Koussoulas N.T, 1998, Differential Petri nets : representing continuous systems in a discrete event world, IEEE-TAC, vol. 43, no. 4, pp. 573 – 579.

Egilmez K., Sharifnia A., 1994, Optimal control of a manufacturing system based on a novel continuous flow model with minimal WIP requirement, Int. Conf. On CIM, pp. 113-118, Albany, USA.

Ghabri M., 1995, Sur la modélisation et la commande des systèmes flexibles de production, Thèse INPG, Grenoble, France.

Giua, A.; DiCesare, F., 1994, Petri net structural analysis for supervisory control., *IEEE Trans. on Robotics and Automation*, Vol. 10, No. 2, pages 185-195.

Hagan M.T., Demuth H., Beale M., 1995, *Neural network design*, PWS publishing company, Boston, U.S.A..

Hanzalek Z., 2003, Continuous Petri nets and polytopes, IEEE-SMC03, pp. 1513-1520, Washington, USA.

Hirasawa K., Ohbayashi M., Sakai S., Hu J., 1998, Learning Petri network and its application to nonlinear system control, *IEEE Trans. on Systems, Man and Cybernetics*, vol. 28, no. 6, pp. 781-789.

Krogh B.H., Kowalewski S., 1996, State feedback control of condition / event systems, *Math. Comput. Modelling*, vol. 23, no. 11/12, pp. 161-173.

Lefebvre D., 1998, A bilinear multimodel approach for the analysis of manufacturing systems, *CESA Proceedings*, vol. 3, pp. 581-584, Hammamet, Tunisie.

Lefebvre D., 1999, Feedback control designs of manufacturing systems modelled by continuous Petri nets, *International Journal of Systems Science*, vol. 30, no. 6, pp. 591-600.

Lefebvre D., 2002, Sensibilité structurelle des réseaux de Petri, 4th International Conference on Applied Mathematics and Engineering Sciences CIMASI02, 23 – 25 octobre, Casablanca, Maroc, CD – ROM.

Lefebvre D, Leclercq E., Draux F., Thomas P., 2003a, Source and sink transitions controllers for continuous Petri nets : a gradient – based approach, IFAC - ADHS03, 16-18 june, Saint Malo, pp. 229 – 234, France.

Lefebvre D, Delherm C., 2003b, Structural sensitivity for the conflicts analysis in Petri nets, IEEE - SMC03, 7-10 october, Washington, USA, CD – ROM.

Lefebvre D, Leclercq E., Draux F., Thomas P., 2004, Commande des flux dans les réseaux de Petri continus par propagation du gradient, CIFA 2004, *invited session SDH (organizer : J. Zaytoon)*, 22 – 24 novembre, Douz, Tunisie

Ljung L., 1987, *System identification: theory for the user*, Prentice Hall, Englewood Cliffs.

Murata T., 1977, State equation, controllability, and maximal matchings of Petri nets, *IEEE Trans. on Automatic Control*, vol. 22, no. 3, pp. 412 – 416.

Murata T., 1989, Petri nets: properties, analysis and applications, *Proceedings IEEE*, vol.77, no. 4, pp 541-580.

Ramadge P.J., Wonham W.M., 1987, Supervisory control of a class of discrete event processes, *SIAM J. Cont. Opt*., vol. 25, pp. 206-230.

Ramchandani C., 1973, *Analysis of asynchronous concurrent systems by timed Petri nets*, Ph. D, MIT, USA.

Sharifnia A., 1994, Stability and performance of distributed production control methods based on continuous flow models, *IEEE Trans. on Automatic Control*, vol. 34, no. 4, pp. 725 – 737.

Sharifnia A., 1988, Production control of a manufacturing system with multiple machine states, *IEEE Trans. on Automatic Control*, vol. 33, no. 7, pp. 620-625.

Silva M., Recalde L., On fluidification of Petri nets : from discrete to hybrid and continuous models, IFAC - ADHS, pp. 9 – 20, 2003

Thomas P., 1997, Contribution à l'identification de systèmes non linéaires par réseaux de neurones, Thèse de Doctorat, Université de Nancy.

Uzam, M.; Jones, A.H.; Yucel, I., 1999, A rule-based methodology for supervisory control of discrete event systems modeled as automation Petri nets, *International Journal of Intelligent Control Systems*, vol. 3, no. 3, pp. 297-325.

Van der Smagt P.P., 1994, Minimisation methods for training feedforward neural networks, *Neural Networks*, vol. 7, no. 1, pp. 1-11.

Widrow B., Lehr M.A., 1990, 30 years of adaptative neural networks: Perceptron, Madaline, and backpropagation, *IEEE Proceedings*, vol. 78, no. 9, pp. 1415-1442.

Zaytoon J., (éditeur), 1998, Hybrid dynamical systems, *APII - JESA*, vol 32, n° 9-10.

Zerhouni N., Ferney M., El Moudni A., 1995, Transient analysis of Petri nets using continuous Petri nets, *Mathematics and Computers in Simulation*, vol. 39, pp. 635 – 639.

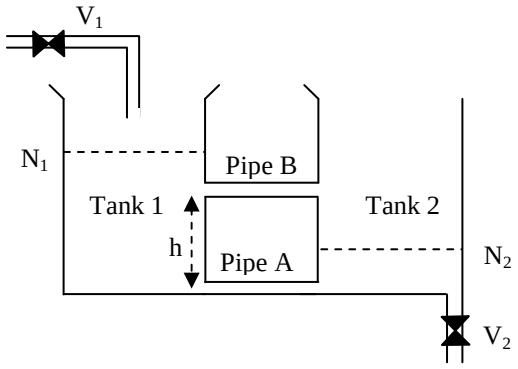

Figure 1: Two tanks system (system A)

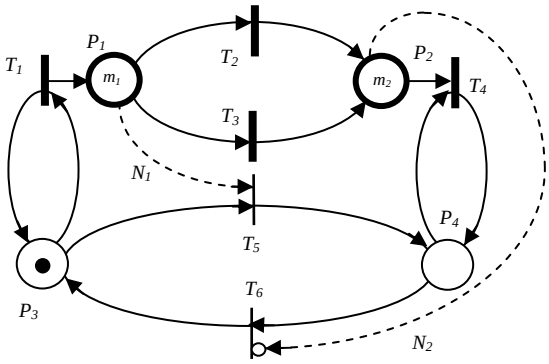

Figure 2: Hybrid PN of the two tanks system

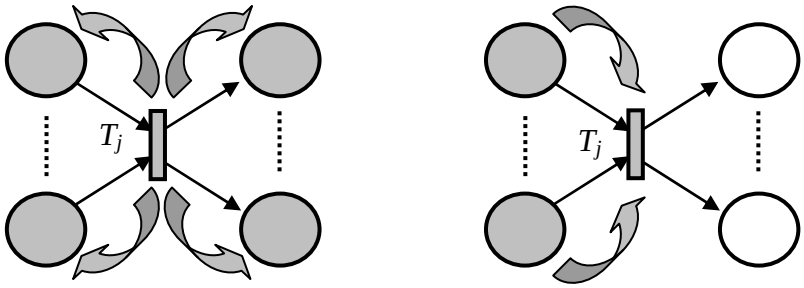

a) Sensitivity of the places next to T_j with respect to the firing conditions of T_j

b) Sensitivity of T_j with respect to the marking of the places next to T_j

Figure 3: Propagation of the perturbation next to the transition T_j

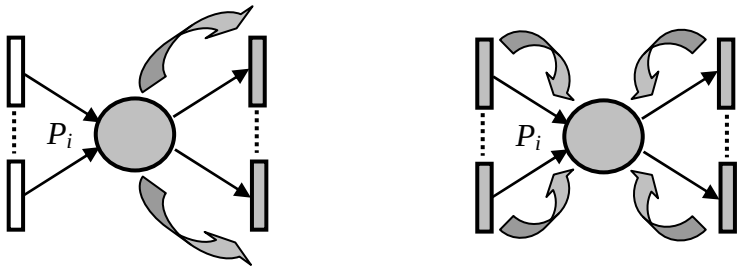

a) Sensitivity of the transitions next to P_i with respect to the marking of P_i

b) Sensitivity of P_i with respect to the firing conditions of the transitions next to P_i

Figure 4: Propagation of the perturbation next to the place P_i

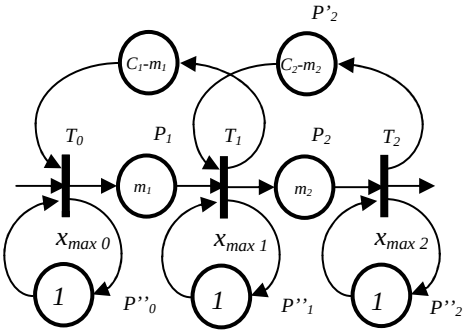

Figure 5: VCPN model of a manufacturing process (system B)

	$A_1(\varphi)$
$C_1 - m_1(t) \geq m''_0(0)$	(1, 0, 0, 0, 0, 0, 0)
$m''_0(0) \geq C_1 - m_1(t)$	(0, 0, 0, 0, 0, 1, 0)

	$B_2(\varphi)$
$m_2(t) \geq m''_2(0)$	(0, 0, 1, 0, 0, 0, 0)
$m''_2(0) \geq m_2(t)$	(0, 0, 0, 0, 1, 0, 0)

	$B_1(\varphi)$
$m_1(t) \geq C_2 - m_2(t) \geq m''_1(0)$	(0, 1, 0, 0, 0, 0, 0)
$C_2 - m_2(t) \geq m_1(t) \geq m''_1(0)$	
$m''_1(0) \geq m_1(t) \geq C_2 - m_2(t)$	(0, 0, 0, 0, 0, 0, 1)
$m_1(t) \geq m''_1(0) \geq C_2 - m_2(t)$	
$C_2 - m_2(t) \geq m''_1(0) \geq m_1(t)$	(0, 0, 0, 1, 0, 0, 0)
$m''_1(0) \geq C_2 - m_2(t) \geq m_1(t)$	

Table 1: Phases specification for system B

$U \setminus Y$	$Y(t) = m_2(t)$	$Y(t) = m_1(t)$	$Y(t) = m_1(t) + m_2(t)$	$Y(t) = (m_1(t), m_2(t))^T$
	$Q = (0\ 0\ 0\ 0\ 1\ 0\ 0)$	$Q = (0\ 0\ 0\ 1\ 0\ 0\ 0)$	$Q = (0\ 0\ 0\ 1\ 1\ 0\ 0)$	$Q = \begin{pmatrix} 0 & 0 & 0 & 1 & 0 & 0 & 0 \\ 0 & 0 & 0 & 0 & 1 & 0 & 0 \end{pmatrix}$
$T_C = \{T_0\}$	$S_W(Y,U) = (1)$	$S_W(Y,U) = (0)$	$S_W(Y,U) = (0)$	$S_W(Y,U) = \begin{pmatrix} 0 \\ 1 \end{pmatrix}$
$T_C = \{T_2\}$	$S_W(Y,U) = (0)$	$S_W(Y,U) = (1)$	$S_W(Y,U) = (0)$	$S_W(Y,U) = \begin{pmatrix} 1 \\ 0 \end{pmatrix}$
$T_C = \{T_0, T_2\}$	$S_W(Y,U) = (1 \quad 0)$	$S_W(Y,U) = (0 \quad 1)$	$S_W(Y,U) = (0 \quad 0)$	$S_W(Y,U) = \begin{pmatrix} 0 & 1 \\ 1 & 0 \end{pmatrix}$

Table 2: Input – output W – sensitivity matrices for system B

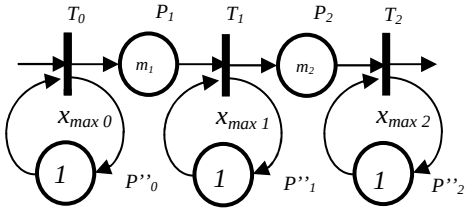

Figure 6: VCPN model of system B'

$U \setminus Y$	$Y(t) = m_2(t)$	$Y(t) = m_1(t)$	$Y(t) = m_1(t) + m_2(t)$	$Y(t) = (m_1(t), m_2(t))^T$
	Q = (0 0 0 0 1)	Q = (0 0 0 1 0)	Q = (0 0 0 1 1 0 0)	$Q = \begin{pmatrix} 0 & 0 & 0 & 1 & 0 \\ 0 & 0 & 0 & 0 & 1 \end{pmatrix}$
$T_C = \{T_0\}$	$S_W(Y,U) = (1)$	$S_W(Y,U) = (0)$	$S_W(Y,U) = (0)$	$S_W(Y,U) = \begin{pmatrix} 0 \\ 1 \end{pmatrix}$
$T_C = \{T_2\}$	$S_W(Y,U) = (0)$	$S_W(Y,U) = (\infty)$	$S_W(Y,U) = (0)$	$S_W(Y,U) = \begin{pmatrix} \infty \\ 0 \end{pmatrix}$
$T_C = \{T_0, T_2\}$	$S_W(Y,U) = (1 \quad 0)$	$S_W(Y,U) = (0 \quad \infty)$	$S_W(Y,U) = (0 \quad 0)$	$S_W(Y,U) = \begin{pmatrix} 0 & \infty \\ 1 & 0 \end{pmatrix}$

Table 3: Input – output W – sensitivity matrices for system B'

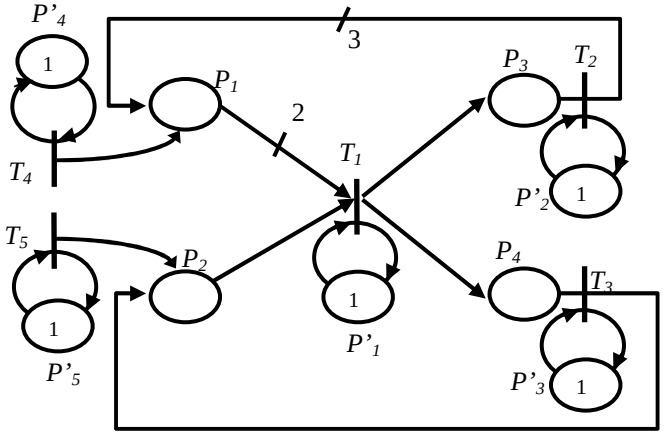

Figure 7: Closed loop process (system C)

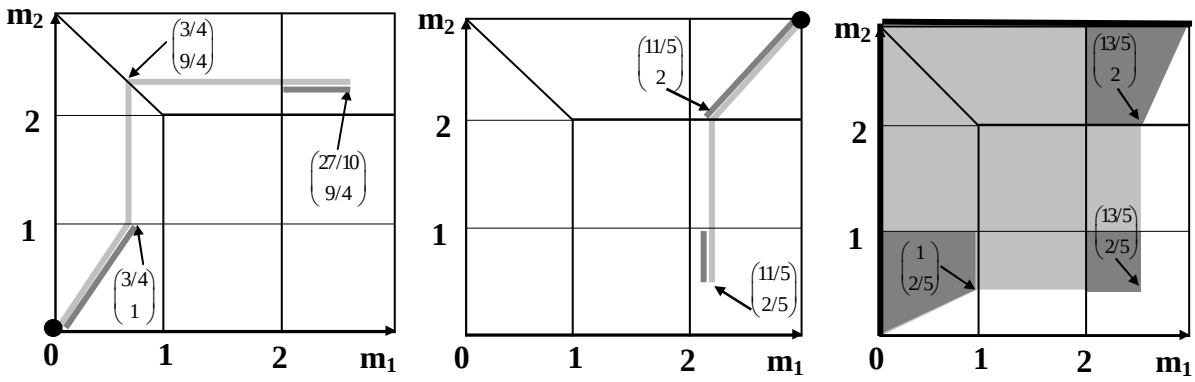

Figure 8: Sets of equilibriums a) $U = x_{max0}$ b) $U = x_{max2}$ c) $U = (x_{max0}, x_{max2})$

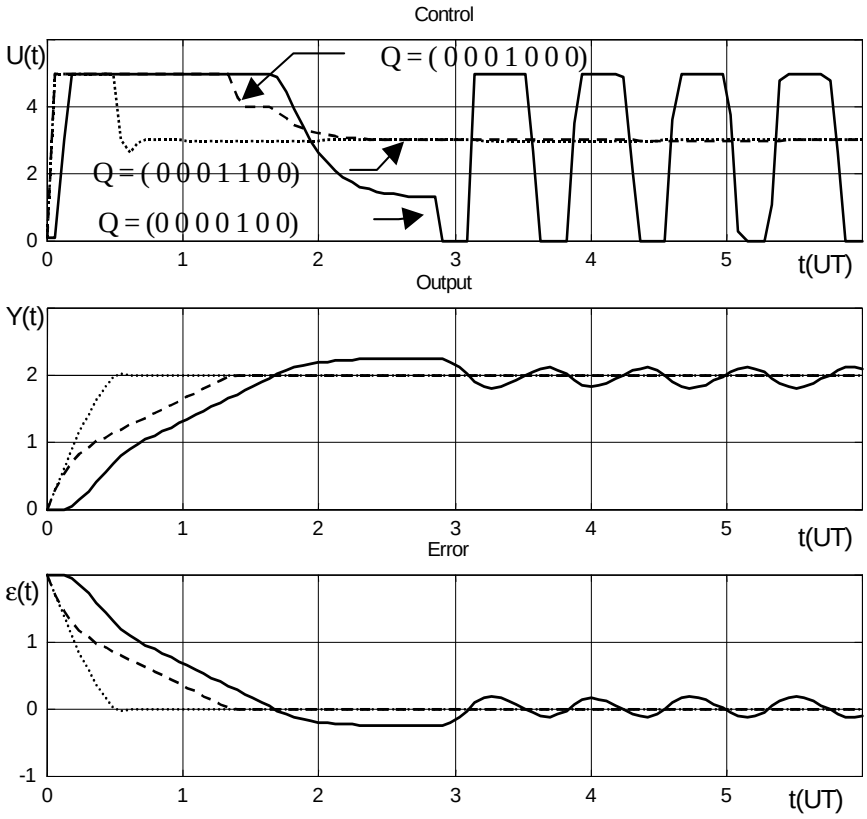

Figure 9: Influence of the output matrix

(full line : Q = (0 0 0 0 1 0 0), dashed line: Q = (0 0 0 1 0 0 0), dotted line Q = (0 0 0 1 1 0 0))

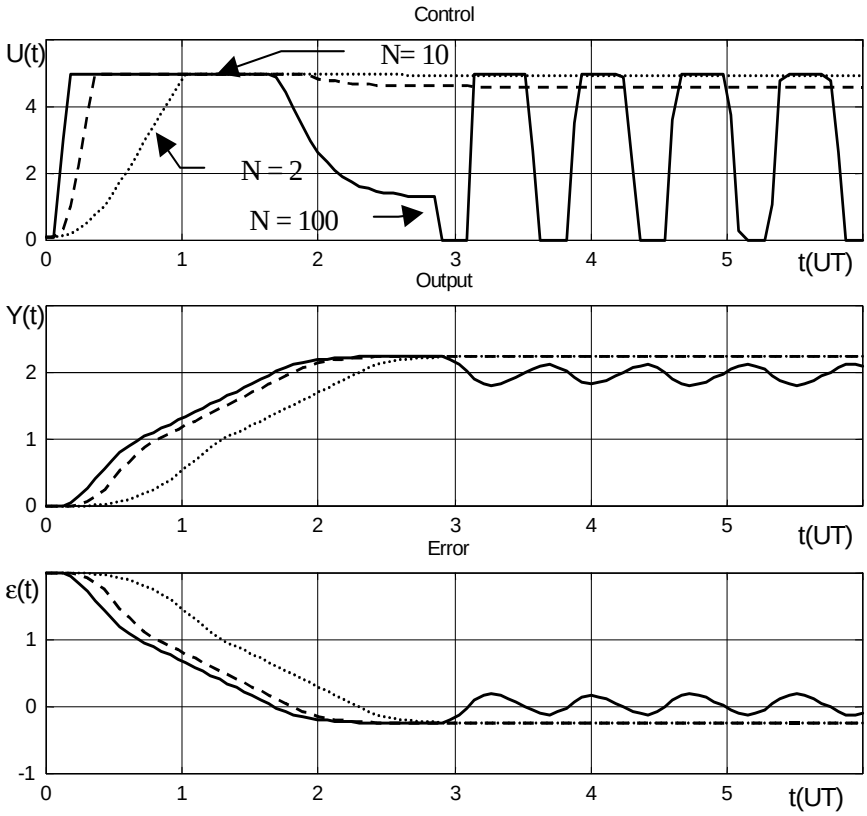

Figure 10: Influence of the iterations number

(full line: $N = 100$, dashed line: $N = 10$, dotted line: $N = 2$)

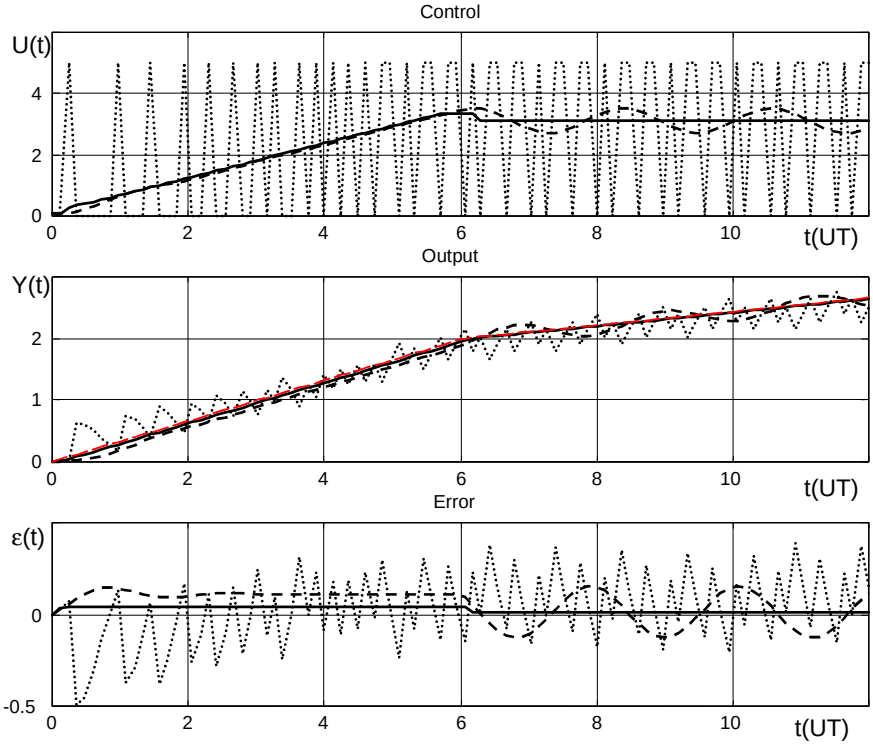

Figure 11: Piecewise linear trajectory
(full line: gradient-based controller, dashed line: proportional controller,
dotted line: bang-bang controller)

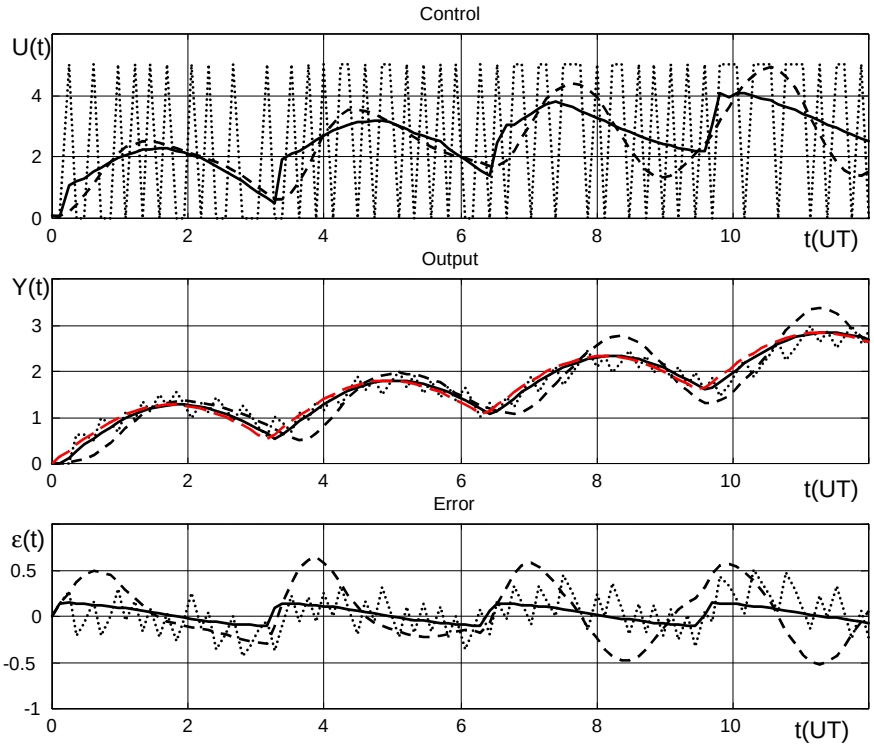

Figure 12: Non linear trajectory

(full line: gradient-based controller, dashed line: proportional controller, dotted line: bang-bang controller)

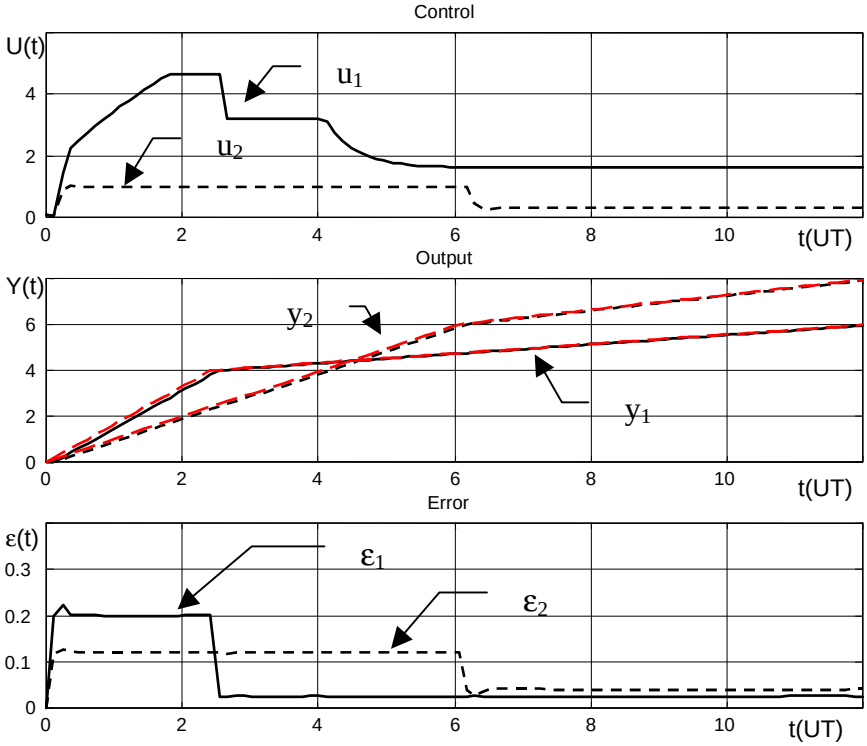

Figure 13: Control design of system C
(full line: first input, first output, dashed line: second input second output)

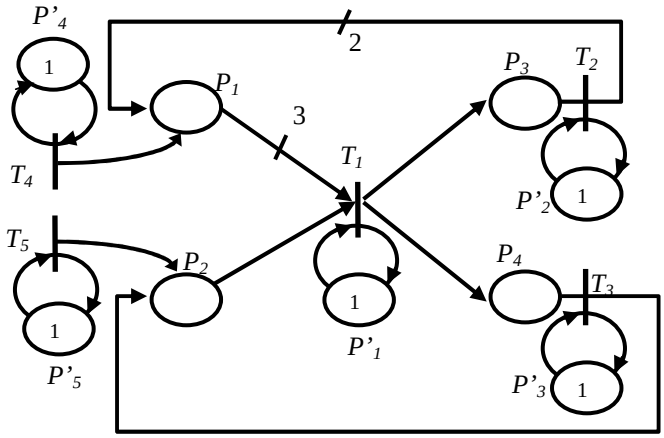

Figure 14: System C'

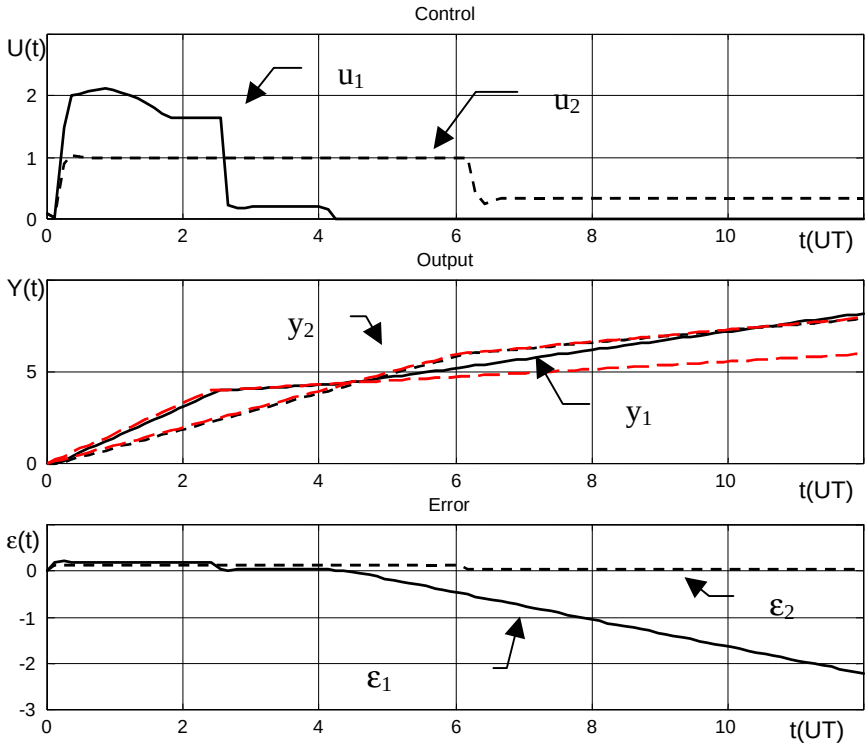

Figure 15: Control design of system C'

(full line: first input, first output, dashed line: second input second output)

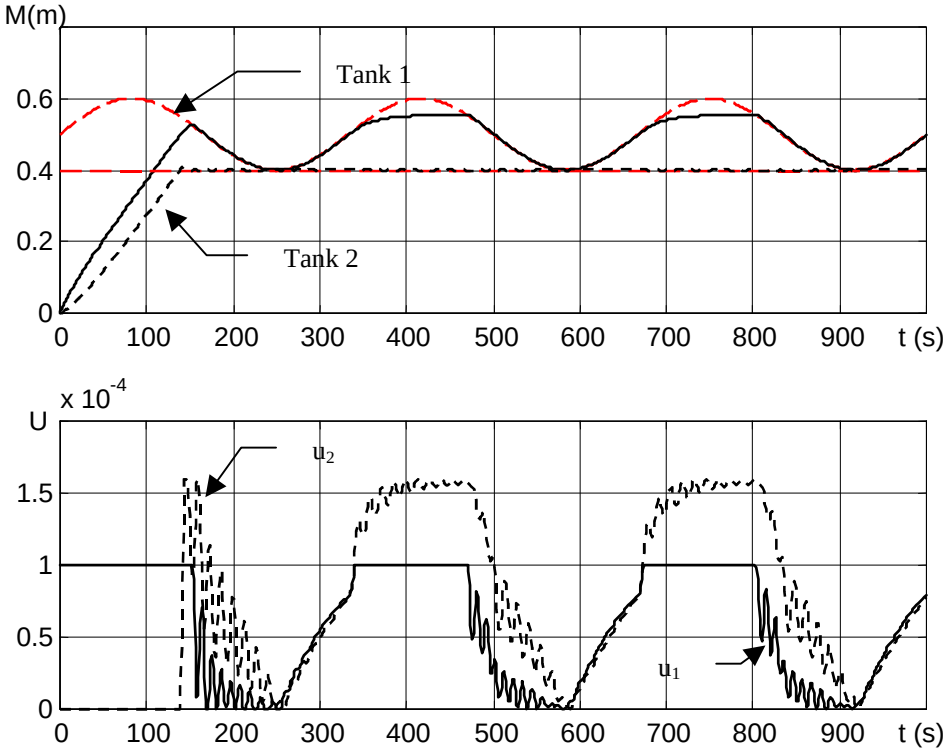

Figure 16: Gradient – based controller for 2 tanks system

(full line: first input, first output, dashed line: second input second output)

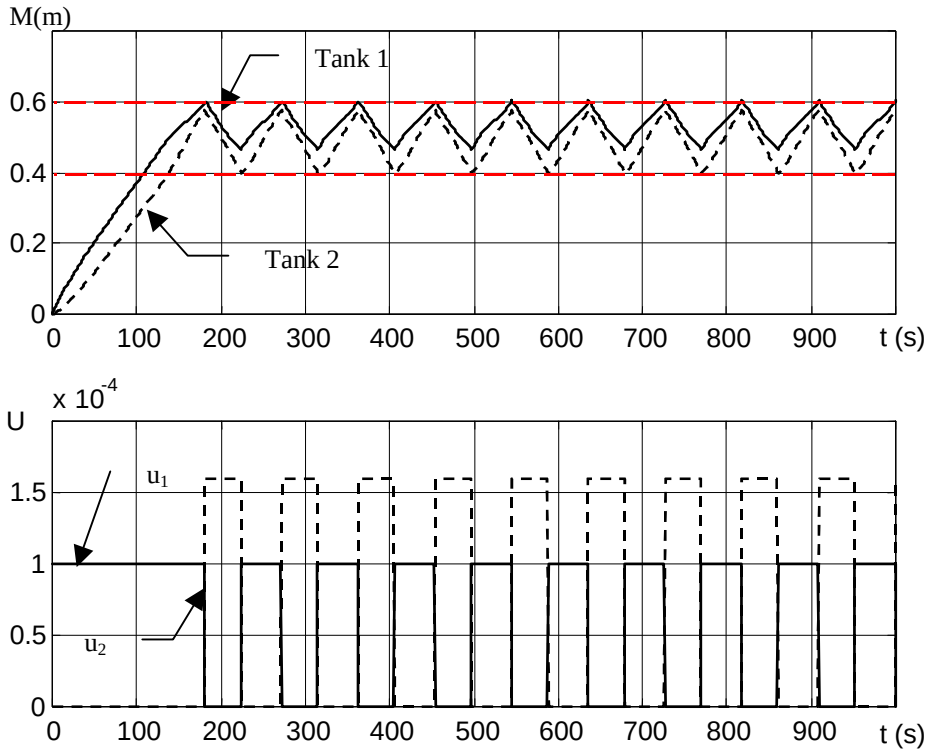

Figure 17: Discrete controller for 2 tanks system

(full line: first input, first output, dashed line: second input second output)

List of figures and tables